

# Optimization of printed sensors to monitor sodium, ammonium, and lactate in sweat

Cite as: APL Mater. **8**, 100905 (2020); <https://doi.org/10.1063/5.0014836>

Submitted: 21 May 2020 . Accepted: 27 September 2020 . Published Online: 15 October 2020

 Alla M. Zamarayeva,  Natasha A. D. Yamamoto,  Anju Toor, Margaret E. Payne, Caleb Woods,  Veronika I. Pister,  Yasser Khan,  James W. Evans, and Ana Claudia Arias

## COLLECTIONS

Paper published as part of the special topic on [Advances in Bioelectronics: Materials, Devices, and Translational ApplicationsBIOE2020](#)



View Online



Export Citation



CrossMark

## ARTICLES YOU MAY BE INTERESTED IN

### Nanopipettes—The past and the present


APL Materials **8**, 100902 (2020); <https://doi.org/10.1063/5.0020011>

### Dynamic excitations of chiral magnetic textures

APL Materials **8**, 100903 (2020); <https://doi.org/10.1063/5.0027042>

### Epitaxial and quasiepitaxial growth of halide perovskites: New routes to high end optoelectronics

APL Materials **8**, 100904 (2020); <https://doi.org/10.1063/5.0017172>



**AMERICAN ELEMENTS**

THE ADVANCED MATERIALS MANUFACTURER®

additive manufacturing epitaxial crystal growth cerium oxide polishing powder silver nanoparticles sputtering targets III-IV semiconductors CVD precursors europium phosphors

deposition slugs OLED Lighting spintronics solar energy osmium nanoribbons thin films chalcogenides AuNPs

GDC Li-ion battery electrolytes 99.999% ruthenium spheres

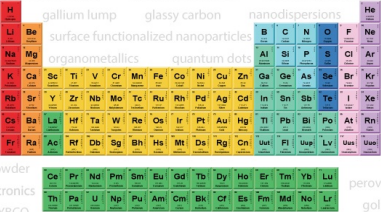
endoheral fullerenes copper nanoparticles diamond micropowder CIGS MBE grade materials palladium catalysts flexible electronics

beta-barium borate borosilicate glass dysprosium pellets YBCO

pyrolytic graphite 3d graphene foam indium tin oxide mesoporous silica

raman substrates sapphire windows tungsten carbide InGaAs

barium fluoride carbon nanotubes lithium niobate scandium powder



gallium lump glassy carbon nanodispersions InAs wafers laser crystals ultra high purity materials MOFs

surface functionalized nanoparticles organometallics quantum dot Al Si P S Cl Ar rare earth metals photovoltaics refractory metals MOCVD

superconductors transparent ceramics ultra high purity silicon

*American Elements opens up a world of possibilities so you can **Now Invent!***

Over 15,000 certified high purity laboratory chemicals, metals, & advanced materials and a state-of-the-art Research Center. Printable GHS-compliant Safety Data Sheets. Thousands of new products. And much more. All on a secure multi-language "Mobile Responsive" platform.

perovskite crystals yttrium iron garnet alternative energy h-BN

gold nanocubes graphene oxide macromolecules photonics

rhodium sponge fiber optics beamsplitters infrared dyes zeolites

fused quartz metallocenes platinum ink buckyballs Ti-6Al-4V

**Now Invent.™**  
The Next Generation of Material Science Catalogs

[www.americanelements.com](http://www.americanelements.com)



# Optimization of printed sensors to monitor sodium, ammonium, and lactate in sweat

Cite as: APL Mater. 8, 100905 (2020); doi: 10.1063/5.0014836

Submitted: 21 May 2020 • Accepted: 27 September 2020 •

Published Online: 15 October 2020



View Online



Export Citation



CrossMark

Alla M. Zamarayeva,<sup>1</sup>  Natasha A. D. Yamamoto,<sup>2</sup> Anju Toor,<sup>2,a)</sup>  Margaret E. Payne,<sup>2</sup> Caleb Woods,<sup>2</sup> Veronika I. Pister,<sup>2</sup>  Yasser Khan,<sup>2</sup>  James W. Evans,<sup>1</sup>  and Ana Claudia Arias<sup>2,b)</sup>

## AFFILIATIONS

<sup>1</sup>Department of Materials Science and Engineering, University of California Berkeley, Berkeley, 2607 Hearst Ave., Berkeley, California 94720, USA

<sup>2</sup>Department of Electrical and Computer Engineering, University of California Berkeley, Berkeley, 2626 Hearst Ave., Berkeley, California 94720, USA

**Note:** This paper is part of the Special Topic on Advances in Bioelectronics.

<sup>a)</sup>Author to whom correspondence should be addressed: [atoor@berkeley.edu](mailto:atoor@berkeley.edu)

<sup>b)</sup>Email: [acarias@berkeley.edu](mailto:acarias@berkeley.edu)

## ABSTRACT

We describe the optimization of a flexible printed electrochemical sensing platform to monitor sodium ion ( $\text{Na}^+$ ), ammonium ion ( $\text{NH}_4^+$ ), and lactate in human sweat. We used previously reported material systems and adapted them to scalable fabrication techniques. In the case of potentiometric  $\text{Na}^+$  and  $\text{NH}_4^+$  sensors, ion-selective electrodes (ISEs) required minimum optimization beyond previously reported protocols, while a reference electrode had to be modified in order to achieve a stable response. We incorporated a carbon nanotube (CNT) layer between the membrane and the silver/silver chloride (Ag/AgCl) layer to act as a surface for adsorption and retention of  $\text{Cl}^-$ . The resulting reference electrode showed minimal potential variation up to 0.08 mV in the solutions with Cl concentration varying from 0.1 mM to 100 mM. Increasing the ionophore content in the  $\text{NH}_4^+$  ISE sensing membrane eliminated an offset in the potential readout, while incorporating CNTs into the sensing membranes had a marginal effect on the sensitivity of both  $\text{Na}^+$  and  $\text{NH}_4^+$  sensors.  $\text{Na}^+$  and  $\text{NH}_4^+$  sensors showed a stable near-Nernstian response with sensitivities of  $60.0 \pm 4.0$  mV and  $56.2 \pm 2.3$  mV, respectively, long-term stability for at least 60 min of continuous operation, and selectivity to  $\text{Na}^+$  and  $\text{NH}_4^+$ . For the lactate sensor, we compared the performance of the tetrathiafulvalene mediated lactate oxidase based working electrode with and without diffusion-limiting polyvinyl chloride membrane. The working electrodes with and without the membrane showed sensitivities of  $3.28 \pm 8$  A/mM and  $0.43 \pm 0.11$   $\mu\text{A}/\text{mM}$  with a linear range up to 20 mM and 30 mM lactate, respectively.

© 2020 Author(s). All article content, except where otherwise noted, is licensed under a Creative Commons Attribution (CC BY) license (<http://creativecommons.org/licenses/by/4.0/>). <https://doi.org/10.1063/5.0014836>

## I. INTRODUCTION

Non-invasive detection of biomarkers in sweat is of great interest for assessing how the body responds to physical activity and for clinical diagnostics. The development of flexible wearable sensors that can be placed in close contact with the skin enables sweat sampling comfortably and quickly as it is secreted out of the skin without contamination or degradation of the analytes.<sup>1</sup> It also allows for the continuous monitoring of biomarkers, enabling the vision of personalized, point-of-care health monitoring.<sup>2</sup>

To date, different sensing methods have been used to build wearable sweat sensors and their components. Impedance-based

sensors have been shown to be effective in monitoring sweat rate<sup>3,4</sup> and could be integrated with sensing components for biomarker monitoring to correct for the effect of sweat rate on the concentration of biomarker. Sensors based on colorimetric readouts were coupled with microfluidic sweat collection and removal systems.<sup>5–9</sup> Optical sweat sensing was also investigated for protein biomarker (e.g., cytokine) and sweat pH detection.<sup>10,11</sup> However, electrochemical sensors gained the most traction due to their high specificity, low cost, and commercially available material systems.<sup>12–14</sup> Compliant wearable sensors for monitoring single<sup>15–24</sup> and multiple<sup>3,10,25–30</sup> analytes in sweat were developed using electrochemical

sensing mechanisms. While the reported work advances the important aspects of sensor development, sensors that meet all the requisites of the commercially viable system are yet to be demonstrated. Such requisites include fast response, sensitivity to physiologically relevant concentrations of analyte, batch to batch reproducibility, stable performance for the duration dictated by the application, specificity, i.e., insensitivity to other analytes present in sweat, long-term storage, and ideally no calibration requirement. Sensor design should also be adapted to fit large scale manufacturing approaches.

In this work, we describe the design and optimization of the flexible printed sensing platform to monitor lactate,  $\text{Na}^+$ , and  $\text{NH}_4^+$  in sweat. Tracking the change in the concentration of these species during the exercise can provide important information for optimizing an individual's sport/fitness routine, as well as for the prevention of complications that could be dangerous to the overall health. Sodium deficit, for instance, is a primary cause of heat cramps<sup>31</sup> and in extreme cases can result in a severe medical condition called hyponatremia. Although the concentration of sodium in sweat is not directly correlated with its plasma concentration, monitoring sodium concentration in sweat can act as a good guide for estimating the loss of this ion in blood and provide guidance regarding the amount of sodium that needs to be replenished. It has been shown that an increased concentration of lactate in sweat is a good indicator of metabolic acidosis, which can develop during prolonged exercise.<sup>32</sup> However, high exertion exercises might lead to an increase in lactate concentration due to the activity of the sweat gland itself and might not correlate with blood lactate.<sup>33,34</sup> A high concentration of ammonia is an indicator of low levels of carbohydrates<sup>35</sup> and can also be an indicator of other metabolic conditions associated with the intense physical performance.<sup>36</sup> Thus, monitoring concentrations of lactate, ammonium, and sodium ions in sweat has benefits, especially for monitoring the effects of prolonged or intense physical activity.

A stable reference electrode is a key requirement for achieving reliable  $\text{Na}^+$  and  $\text{NH}_4^+$  potentiometric sensors. The reference electrode for potentiometric sensors should be insensitive to the changes in chloride ion ( $\text{Cl}^-$ ) concentration. Such printed reference electrodes are conventionally achieved by depositing polymeric membrane saturated with chloride salt on top of the Ag/AgCl layer.<sup>37–42</sup> Polyvinyl butyral (PVB)/sodium chloride (NaCl) membrane drop-casted on top of the Ag/AgCl layer has been widely used for wearable potentiometric sensors.<sup>16,23,27,29,43–47</sup> Using a reference electrode based on PVB polymer for wearable potentiometric sensors was first explored by Guinovart *et al.*<sup>38</sup> and was consequently widely adopted partially due to its straightforward fabrication protocol. The PVB reference solution is prepared by dissolving PVB and NaCl into methanol, mixing, and then casting the PVB reference solution onto the Ag/AgCl electrodes. The general issue with such electrodes is that when submerged in aqueous solutions, chloride ions tend to diffuse from the membrane into the solution. The concentration of  $\text{Cl}^-$  decreases, which in turn leads to the drift in potential, thus compromising the stability of the sensor readout. To achieve a stable response, Guinovart *et al.* performed a preliminary conditioning step, where the electrodes were immersed in 3M KCl for 12 h.<sup>38</sup> While conditioning has a favorable influence on the stability of the electrode in different electrolyte concentrations, requirement for prolonged conditioning complicates the manufacturing/usability

of the sensors for wearable applications. The consequent literature reports on wearable potentiometric sensors with the PVB-based reference rarely report data for the characterization of the reference electrode or continuous sensor operation for at least 60 min without the potential drift.<sup>16,23,29,44,45</sup> To mitigate the diffusion of the chloride ions, we incorporated a carbon nanotube (CNT) layer between the membrane and the Ag/AgCl layer to act as a surface for the adsorption and retention of chloride ions. This effective modification led to a stable, reproducible reference electrode. Coupling the reference electrode with ion-selective electrodes (ISEs) for  $\text{Na}^+$  and  $\text{NH}_4^+$  enabled printed wearable potentiometric sensors with a near-Nernstian response. The sensors showed stable response when continuously operated for 60 min and required minimum optimization beyond previously reported protocols. Particularly, adding different weights fractions of CNTs into the sensing membrane of ISEs resulted in a marginal improvement in the electrochemical performance. This is in contrast to the literature reports where CNTs are incorporated into the sensing membrane of potentiometric sensors to act as an ion to electron transducer.<sup>48–50</sup>

Optimization of the working electrode constitutes the most significant effort for realizing an amperometric lactate sensor. We compared the performance of the lactate working electrode with and without diffusion-limiting PVC membrane. A diffusion-limiting membrane is important because the enzymatic reaction is fast, and the rate at which the lactate is reduced to pyruvate at the working electrode, and thus, the sensor response is limited by a mass transfer of lactate to the electrode surface. Mass transfer, in turn, is determined by the bulk concentration of lactate, area of the electrode, diffusion, and convection.<sup>51</sup> For the applications considered in this work, the wearable sensor needs to be placed directly on the skin and continuously measure lactate concentration under the variable sweat flow rate for the duration of an exercise. Therefore, the transport of lactate to the electrode surface would be challenging to control. The membrane ensures that the sensor response is unaffected by the motion of sweat since diffusion within the membrane is significantly lower than the external diffusion.<sup>52</sup> Furthermore, in our previous work, we showed that biologically relevant concentrations of sodium, potassium, and calcium ions present in sweat affect the enzyme activity and, thus, the sensitivity of the lactate sensors.<sup>53</sup> The membrane reduces the relative variation of the sensor's sensitivity with respect to variations of the enzyme activity.<sup>53</sup> The 3 mm diameter electrodes with and without the membrane showed sensitivities of 3.28  $\mu\text{A}/\text{mM}$  and 0.43  $\mu\text{A}/\text{mM}$  with a linear range up to 20 mM and 30 mM lactate, respectively.

## II. RESULTS AND DISCUSSION

We employed scalable fabrication methods such as inkjet printing, screen printing, and drop-casting for the fabrication of the sweat sensor platform. Lactate is monitored through amperometric measurements that require a three-electrode setup. The potential is set between the working and reference electrode to facilitate the electrochemical reaction between the enzyme lactate oxidase present in the working electrode and lactate in sweat. The resulting current is then detected. Potentiometric measurements of sodium ion and ammonium ion are performed by measuring the potential difference between reference and ion selective electrodes, thus requiring a two-electrode design. ISEs are composed of ionophores that reversibly

bind  $\text{Na}^+$  and  $\text{NH}_4^+$  ions, ideally resulting in a Nernstian response to the change in ion concentration. Figure 1(a) shows the schematic of the sweat sensing platform consisting of a three-electrode lactate sensor and two-electrode  $\text{Na}^+$  and  $\text{NH}_4^+$  sensors sharing the same reference electrode.

### A. Sensor fabrication

Working transducer electrodes for both potentiometric and amperometric sensors, as well as the counter electrode for the amperometric sensor, were fabricated by inkjet printing commercially available gold nanoparticle ink onto 25  $\mu\text{m}$  thick PEN substrates [Fig. 1(b)]. The 25  $\mu\text{m}$  PEN substrate was chosen due to its conformability to the skin and its ability to withstand the sintering temperature of gold nanoparticle ink (250 °C). The reference electrodes for the potentiometric and amperometric sensors consisted of commercial Ag/AgCl ink, screen-printed onto the same substrate [Figs. 1(c) and 1(d)]. Figure S1 in the [supplementary material](#) shows the scanning electrode microscope images of the top and side view of the screen-printed Ag/AgCl trace. In the case of the potentiometric sensors, an additional layer of CNTs dispersed in tetrahydrofuran (THF), followed by a polyvinyl butyral (PVB)/sodium chloride (NaCl) membrane, was drop-cast on top of the Ag/AgCl layer. The sensing membranes for the sodium and ammonium working electrodes were prepared by drop-casting the respective ionophore solutions or ionophore/CNT suspensions onto the gold working electrodes. The working electrode for the lactate sensor consists of the mediating layer, fabricated by drop-casting CNT/TTF suspension onto the gold electrode (3 mm diameter), followed by lactate oxidase enzyme immobilized in the chitosan/CNT suspension.

### B. Optimization of $\text{Na}^+$ and $\text{NH}_4^+$ potentiometric sensors

Potentiometric sensors rely on the determination of the potential between ion-selective and reference electrodes. The reliable performance of these sensors highly depends on the stability of the reference electrode in different ionic environments. The reference electrode is conventionally achieved by depositing a polymeric membrane saturated with the chloride salt on top of the printed Ag/AgCl traces.<sup>15,29,30,54,55</sup>

#### 1. Reference electrode

To determine the optimum thickness of the Ag/AgCl traces, we compared the performance of the screen-printed traces with three thicknesses: 12  $\mu\text{m}$ , 25  $\mu\text{m}$ , and 50  $\mu\text{m}$ . Figure 2(a) shows the potential response of the 12  $\mu\text{m}$  (red), 25  $\mu\text{m}$  (green), and

50  $\mu\text{m}$  (black) Ag/AgCl traces tested against a single junction commercial Ag/AgCl reference in concentrations of NaCl solution ranging from  $10^{-4}$  M to  $10^{-1}$  M. The linear fit for the response of the corresponding electrodes is shown in Fig. 2(b). Ag/AgCl traces show fast, reversible response with sensitivities of 56.6 mV/decade, 55.5 mV/decade, and 54.2 mV/decade for the 12  $\mu\text{m}$ , 25  $\mu\text{m}$ , and 50  $\mu\text{m}$  thick electrodes, respectively. Thus, Ag/AgCl traces with thickness in the 12  $\mu\text{m}$ –50  $\mu\text{m}$  range show behavior close to the ideal Nernstian behavior (59 mV/decade). However, thinner electrodes are preferred for improved flexibility, and therefore, 12  $\mu\text{m}$  Ag/AgCl traces were used to fabricate printed reference electrodes.

To make the reference electrode insensitive to the change in Cl concentration, we combined the Ag/AgCl layer with a PVB membrane.<sup>38</sup> The thickness of the membrane is an important parameter in the electrode architecture. The membrane must be thick enough to maintain a high concentration of the chloride ions at the electrode surface and prevent the efflux of the ions into the external solution. At the same time, an electrode with a thicker membrane might require extensive conditioning to achieve stable response. The potential response of the reference electrodes with different membrane thicknesses to change in the concentration of NaCl solution is presented in Fig. S2(a). Varied volumes of PVB solution were deposited to obtain membranes of different thicknesses. Reference electrodes are not sensitive to changes in concentrations below values of  $10 \times 10^{-3}$  M. The electrodes exhibited a linear response in the region of higher concentration values with a slope of  $-11$  mV/decade,  $-35$  mV/decade, and  $-37$  mV/decade for the membranes formed from 10  $\mu\text{l}$ , 8  $\mu\text{l}$ , and 4  $\mu\text{l}$  of the polymer solution, respectively. Thicker electrode membranes were less sensitive to the change of salt concentration. However, increasing thickness of the membrane resulted in longer equilibration time, as confirmed by Figs. S2(b) and S2(c) showing the corresponding potential readouts for the electrodes with 4  $\mu\text{l}$  and 8  $\mu\text{l}$  membranes. The electrodes were immersed in solutions of different NaCl concentrations and the response was recorded for 10 s following the immersion. Electrodes with 8  $\mu\text{l}$  membranes show poor reversibility and delayed response. Therefore, incorporating the PVB membrane on the reference electrode was ineffective for achieving electrode stability, likely due to the diffusion of chloride ions from the membrane into the solution.

To improve the reference electrode stability, we modified the PVB membrane using CNTs. CNTs have been previously incorporated into the membrane of the reference electrode to achieve stable response.<sup>27,29,47</sup> CNT layer can act as a surface for Cl adsorption and, thus, facilitate the retention of the ions at the electrode surface. We tested two approaches: in the first case, CNTs were

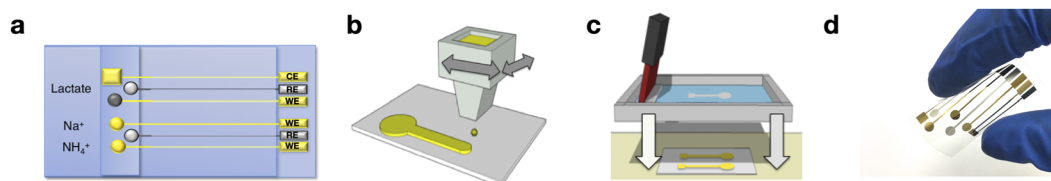


**FIG. 1.** (a) Schematic of the sweat sensing platform. Schematic of the (b) inkjet printing and (c) screen printing. (d) Image of the PEN substrate with inkjet printed gold transducer and screen printed Ag/AgCl reference electrodes.

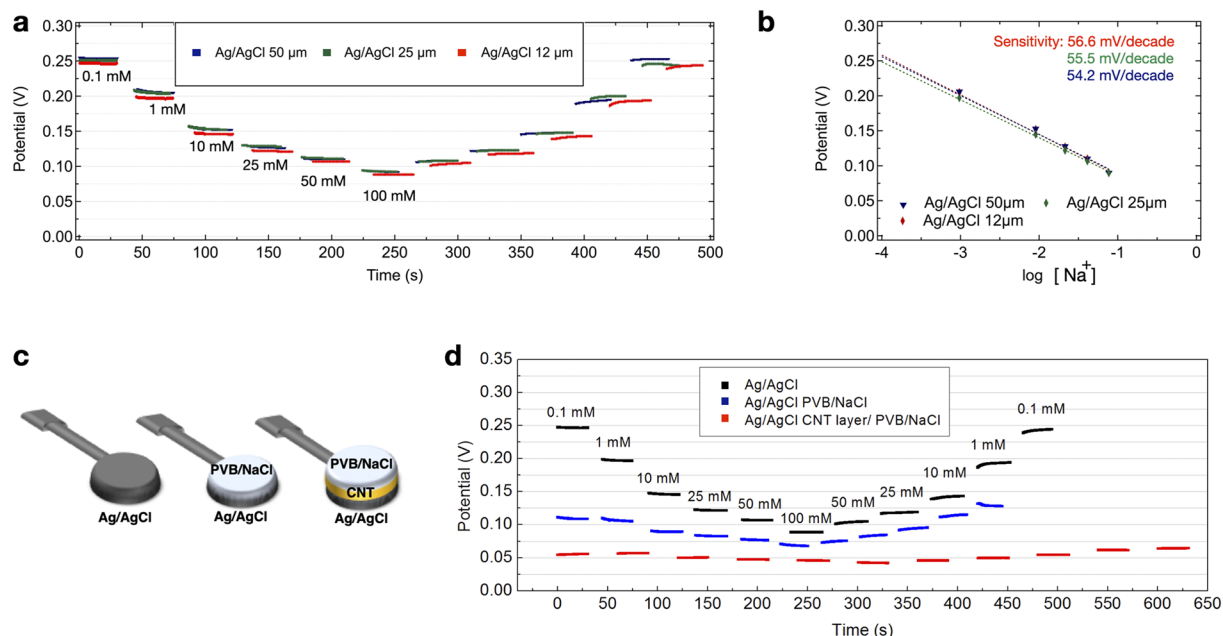


**FIG. 2.** Potential response (a) and the corresponding linear fit (b) of the 12  $\mu\text{m}$ , 25  $\mu\text{m}$ , and 50  $\mu\text{m}$  screen printed Ag/AgCl traces tested against a single junction commercial Ag/AgCl reference in concentrations of NaCl solution ranging from  $10^{-4}$  M to  $10^{-1}$  M. (c) Schematic and (d) comparison of sensitivity to changes in the NaCl concentration of the reference electrodes fabricated with CNTs dispersed in the membrane (blue), the electrodes with the CNT layer (red), and electrodes without the membrane (black).

dispersed in the membrane of the reference electrode; in the second case, a CNT layer was created between the membrane and Ag/AgCl. In order to form a CNT layer, homogeneous CNT/THF suspension was obtained using the block copolymer PEO-PPO-PEO (F127) as a surfactant, and then the resulting suspension was deposited via drop-casting to form the layer. Figure 2(c) shows the schematics and Fig. 2(d) compares the sensitivity to changes in the NaCl concentration of the reference electrodes fabricated with CNTs dispersed in the membrane (blue), the electrodes with the CNT layer (red), and electrodes without a membrane (black). Reference electrodes fabricated with CNTs dispersed in the membrane exhibit an unstable response in the region of lower (0.1 mM–1 mM) NaCl concentrations and show a linear response in the region of higher (10 mM–100 mM) salt concentrations, with overall variations in the potential ranging from 0.08 mV to 0.13 mV. The electrodes with the CNT layer show a significantly improved constancy with the overall potential variation ranging between 0.075 mV and 0.08 mV. Thus, by introducing a CNT layer between the PVB membrane and the Ag/AgCl layer, we obtained a reference electrode with minimal sensitivity to variations in the concentration of the NaCl solution.

## 2. Sensing electrode

Coupling the reference electrode with ISEs for  $\text{Na}^+$  and  $\text{NH}_4^+$  enabled printed wearable potentiometric sensors with a near-Nernstian response [Fig. 3(a)]. ISEs were prepared by first combining ion-selective ionophore solutions or ionophore/CNT suspensions with PVC as a polymer additive and then drop-casting onto the gold transducer electrodes to form ion-selective

membranes. Ionophores reversibly bind  $\text{Na}^+$  or  $\text{NH}_4^+$  ions, ideally resulting in a Nernstian response, i.e., demonstrate a sensitivity of 59.1 mV/decade, i.e., a 59.1 mV change for every factor of ten change in the concentration of the ion.

While sensing electrodes for the potentiometric sensors require minimum optimization beyond previously reported protocols for sensor fabrication, tuning ionophore content in the sensing membrane further improved the sensor performance. Figures 3(b) and 3(c) show the calibration curves of the  $\text{NH}_4^+$  sensing electrodes with 3% and 0.2% ionophore content tested against a commercial reference electrode, respectively. Concentrations of  $\text{NH}_4\text{Cl}$  solution varied between  $10^{-5}$  M and  $10^{-1}$  M. Both types of ion-selective electrodes showed a near-Nernstian response. Electrodes with 0.2% ionophore showed an offset of 0.1 V in the potential read-out. The offset can be accounted for by calibrating sensors before use, but calibration is overall undesirable for the wearable sensor devices.

## 3. Sensitivity and detection range

Since CNTs can serve as an effective ion to electron transducers,<sup>48–50</sup> we also studied the effect of adding different weight fractions of CNTs into the sensing membrane of ISEs. For this study, we employed the optimized reference electrodes (as discussed in Sec. II B 1) that comprise a CNT layer between the reference PVB membrane and the Ag/AgCl layer. Figure 3 compares the open circuit potentials and calibration curves of [(d)–(f)] sodium and [(g)–(i)] ammonium sensors with 0% and 2% CNTs dispersed in the sensing membrane. Concentrations of the NaCl solution varied from  $10^{-3}$  M to  $10^{-1}$  M and concentrations of the  $\text{NH}_4\text{Cl}$  solution

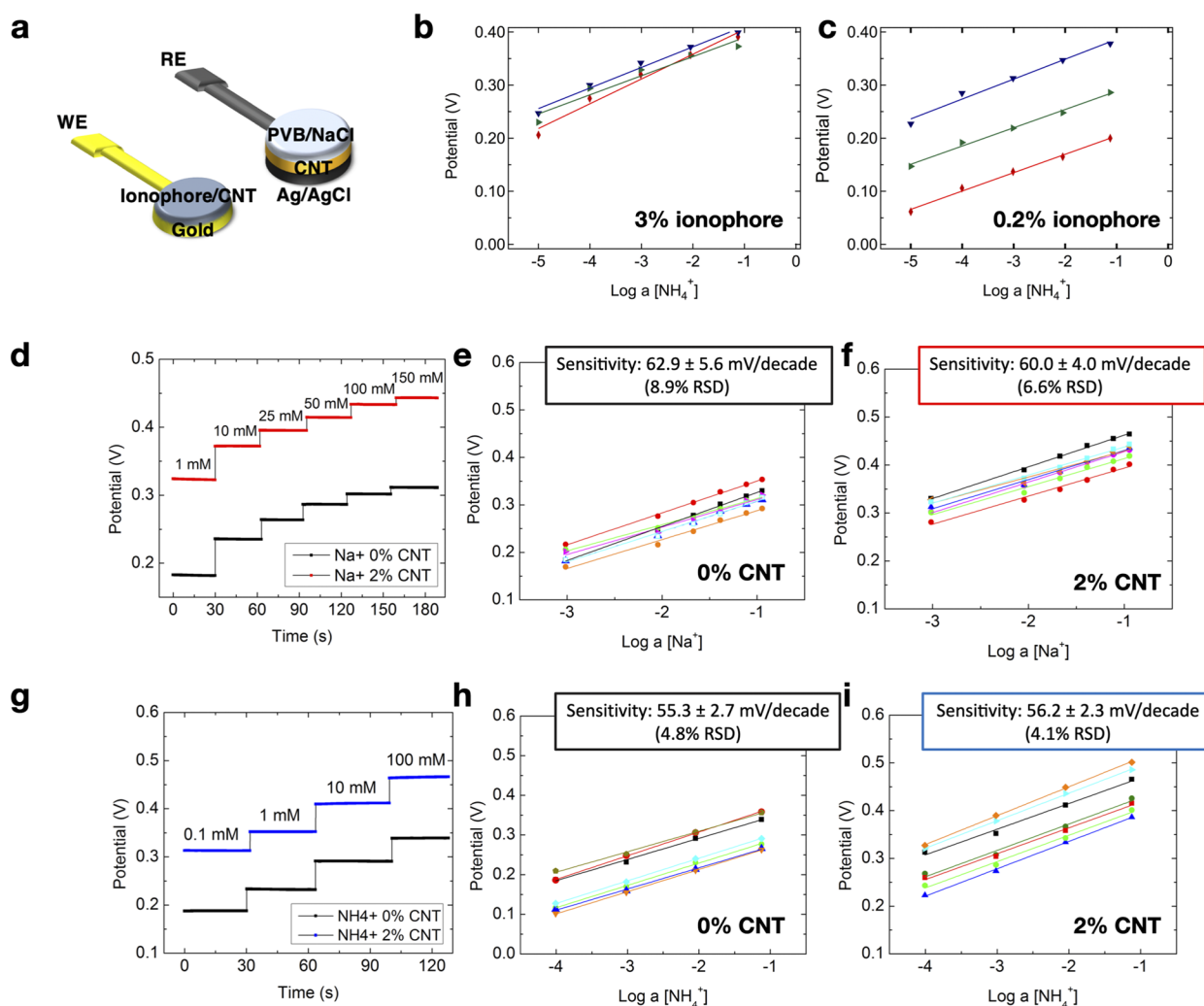


**FIG. 3.** (a) Schematic of the potentiometric sensor. Calibration curves of the  $\text{NH}_4^+$  sensing electrodes with (b) 3% and (c) 0.2% ionophore content tested against commercial reference and counter electrodes. [(d) and (g)] Open circuit potentials and [(e), (f), (h), and (i)] calibration curves of [(d)–(f)]  $\text{Na}^+$  and [(g)–(i)]  $\text{NH}_4^+$  sensors with [(c) and (f)] 0% and [(b) and (e)] 2% CNTs dispersed in the sensing membrane in the electrolyte solutions with physiologically relevant concentrations of the corresponding ions. Concentrations of the NaCl solution varied from  $10^{-3}$  M to  $10^{-1}$  M, and concentrations of the  $\text{NH}_4\text{Cl}$  solution varied from  $10^{-4}$  M to  $10^{-1}$  M.

varied from  $10^{-4}$  M to  $10^{-1}$  M. Sodium sensors with 2% and 0% of CNTs had sensitivities of  $60.0 \pm 4.0$  mV/decade ( $N = 7$ ) and  $62.9 \pm 5.6$  mV/decade ( $N = 7$ ), respectively. Ammonium sensors had sensitivities of  $55.3 \pm 2.7$  mV/decade ( $N = 8$ ) and  $56.2 \pm 2.3$  mV/decade ( $N = 8$ ) for sensors with 0% and 2% CNTs, respectively. The addition of CNTs in the sensing membrane resulted in a marginal improvement in sensitivity and response time. ISEs with 2% CNTs showed the least variability in response to varied salt concentrations (Fig. S3).

While previous studies were successful in achieving potentiometric  $\text{Na}^+$  or  $\text{NH}_4^+$  sensors with a near-Nernstian behavior,<sup>7,16,23,29,44,45</sup> the stability under continuous operation for at least 60 min was rarely reported. Figures 4(a) and 4(b) show the long-term potential response of the ammonium [Fig. 4(a)] and the

sodium [Fig. 4(b)] sensors with 0% and 2% CNTs content in the sensing membrane when continuously operated for 60 min.  $\text{Na}^+$  and  $\text{NH}_4^+$  sensors were tested in 50 mM NaCl and 1 mM  $\text{NH}_4\text{Cl}$  solutions, respectively, representing the averages of the physiologically relevant concentrations of the corresponding ions in sweat. The sensors were conditioned for 25 min before the measurement. All sensors showed a stable long-term stability for at least 60 min of operation, which is the average duration of the workout. The CNT content did not seem to affect the sensor stability.

#### 4. Selectivity analysis

Sweat is rich with a plethora of ions, and it is important to ensure that they do not interfere with sensor response. Figures 4(c) and 4(d) show the selectivity of the ammonium [Fig. 4(c)] and

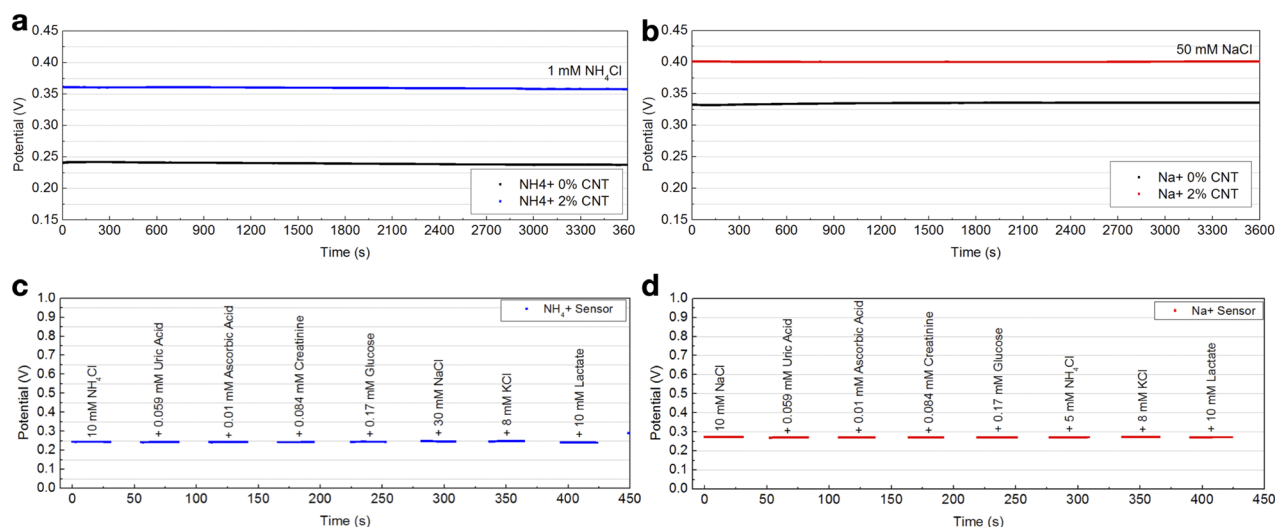


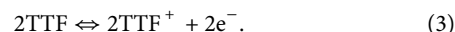
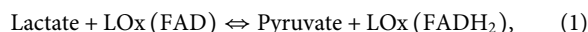
**FIG. 4.** [(a) and (b)] Long term stability of the (a) NH<sub>4</sub><sup>+</sup> and (b) Na<sup>+</sup> sensors without CNTs and 2% CNTs dispersed in the sensing membrane. [(c) and (d)] Selectivity of the (c) NH<sub>4</sub><sup>+</sup> and (d) Na<sup>+</sup> and sensors without CNTs in the sensing membrane.

sodium [Fig. 4(d)] sensors without CNTs in the sensing membrane. Here, we measure the Na<sup>+</sup> and NH<sub>4</sub><sup>+</sup> sensors' response in the solutions of the respective Na<sup>+</sup> and NH<sub>4</sub><sup>+</sup> ions while adding physiologically relevant concentrations of the standard ionic interfering species found in sweat—K<sup>+</sup> and NH<sub>4</sub><sup>+</sup> for Na<sup>+</sup> sensor, Na<sup>+</sup> and K<sup>+</sup> for NH<sub>4</sub><sup>+</sup> sensor, as well as physiologically average amounts of sweat components—creatinine, glucose, uric acid, and ascorbic acid. Solutions of 8 mM KCl and 30 mM NaCl were added to the 10 mM solution with NH<sub>4</sub><sup>+</sup> sensor. Similarly, for Na<sup>+</sup> sensor, solutions of 8 mM KCl and 5 mM NH<sub>4</sub>Cl were added to the 10 mM NaCl solution, followed by adding 0.084 mM creatinine, 0.17 mM glucose, 0.059 mM uric acid, and 0.01 mM ascorbic acid to solutions with both sensors. These species introduced a minimal variation in sensor potential, indicating no interference. Additionally, we compared the performance of Na<sup>+</sup> sensor in the solutions of NaCl in artificial sweat comprised from the aforementioned species with that in water and did not observe a statistically significant difference in sensitivity (Fig. S4).

### C. Characterization of the working electrode for the printed flexible lactate sensor

The design and optimization of the working electrode constitutes the most significant effort in the lactate sensor development. Figure 5(a) shows the schematics of the working electrode. It consists of three layers sequentially deposited onto the flexible substrate. The top layer comprises sensing component (LOx) immobilized in the polysaccharide chitosan to prevent its efflux into the sweat. The bottom layer is a gold transducer electrode. The mediating layer, composed of a TTF mediator and CNTs, is incorporated between LOx and the transducer. We chose TTF due to its well-characterized performance in enzymatic sensors<sup>55–57</sup> and compatibility with dermal applications.<sup>15</sup>

When the lactate from sweat comes in contact with the enzyme on the electrode, the flavin adenine dinucleotide (FAD) of the enzyme oxidizes it to pyruvate, while the dinucleotide itself gets reduced. The enzyme is then oxidized back to its original form by TTF<sup>+</sup>, at the same time TTF<sup>+</sup> is reduced to TTF. Then it is converted back to TTF<sup>+</sup> on the electrode. Two electrons are produced as a result of this reaction, as shown in Eqs. (1)–(3). Thus, the detected current is directly proportional to the concentration of lactate,



The system's redox potentials vary depending on the composition of the electrode. Overall, to avoid interference from electroactive species in sweat, the applied positive potential should not exceed 0.45 V.<sup>56</sup> We determine the operating potential of the working electrode through cyclic voltammetry (CV). To reduce the number of variables, we used a commercially available silver/silver chloride (Ag/AgCl) electrode as a reference and platinum wire as a counter electrode.

Figure 5(b) shows the CV plots for the mediated working electrodes tested with and without the presence of lactate. The curve without lactate (red) has one oxidation (top) and one reduction (bottom) peak corresponding to the oxidation and reduction of TTF. On the addition of lactate, the oxidation peak increases in size, while reduction peak decreases. The oxidation peak increases because the lactate in the solution is oxidized in addition to TTF contributing to the higher current. The reduction peak is reduced because reaction (3) (right to left) is inhibited by larger amounts of TTF that are present, because the reaction in Eq. (2) is also inhibited by large

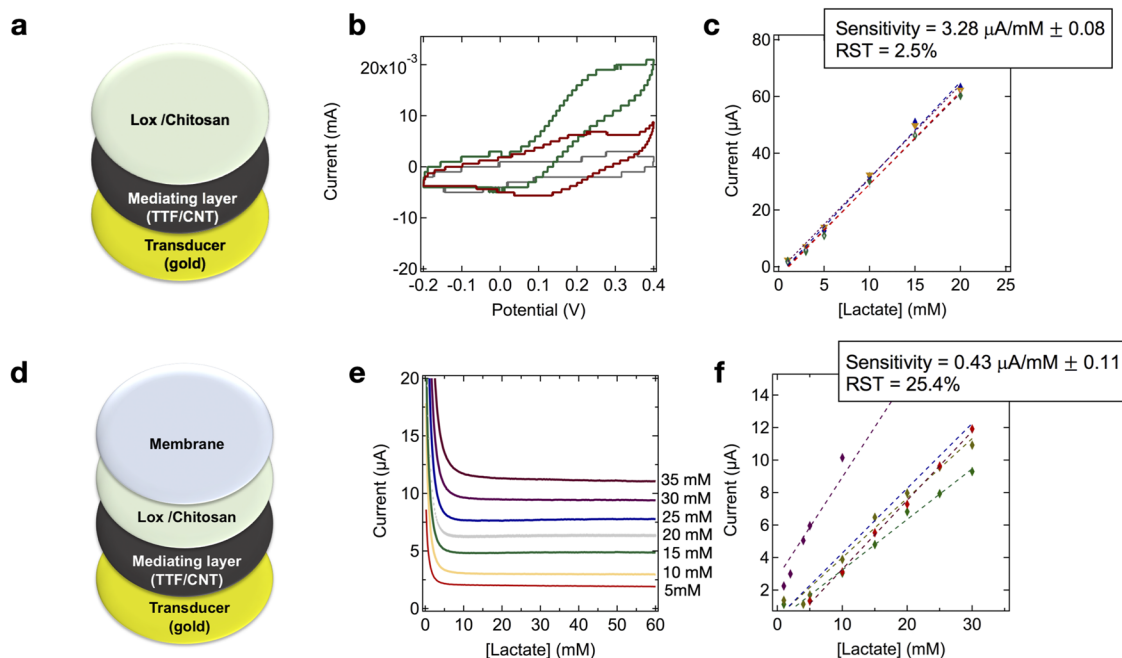


**FIG. 5.** Schematics of the lactate sensor working electrode components (a) without and (d) with the diffusion limiting membrane. (b) CV plots for the mediated working electrodes tested with (green) and without (red) the presence of lactate, and CV plot of the unmediated electrode (gray). (c) Calibration curves of the four lactate working electrodes without the membrane. (e) Chronoamperometric response to increasing lactate concentrations from 5M to 35M in the increments of 5M. (f) Calibration curves of the five lactate working electrodes with the diffusion limiting membrane.

amounts of Lox(FADH<sub>2</sub>) caused by reaction (1). The maximum current is achieved at  $\sim 0.2$  V, which is significantly lower than the theoretical 0.6 V required to operate the sensor without TTF.<sup>58</sup> The gray curve of Fig. 5(b) confirms that the electrode fabricated without TTF and operated in the same potential range is unresponsive to the addition of lactate. Therefore, in the consequent measurements, electrodes were fabricated with TTF mediator and 0.2 V potential step (vs Ag/AgCl commercial reference) was used for the measurement of sensor sensitivity.

Figure 5(c) shows the calibration curves of four lactate working electrodes without the membrane. The electrodes had a linear range up to 20 mM and the sensitivity of  $3.28 \pm 8 \mu\text{A}/\text{mM}$  for a 3 mm diameter electrode. The response of the electrodes was highly reproducible with the relative standard deviation of 2.5%. Furthermore, the sensitivity of the fully printed sensor is in good agreement with that of the working electrode tested with commercially available counter and reference electrodes [Fig. S5(a)]. The sensor shows a stable performance for at least an hour of continuous operation [Fig. S5(b)].

We then characterized the performance of the same working electrode after incorporating a diffusion limiting membrane [Fig. 5(d)]. We used PVC, a polymer widely utilized to fabricate sweat sensor components,<sup>15,29,30,54,55</sup> as a membrane material. The PVC membrane was drop-casted from the solution on top of the electrode. Figure 5(e) shows the chronoamperometric response of the working electrode to increasing lactate concentrations from 5 mM to 35 mM in increments of 5 mM. The electrode shows a fast

stable response reaching a steady state after  $\sim 10$  s. Figure 5(f) shows the calibration curves of the five lactate working electrodes with the diffusion limiting membrane. Incorporating the membrane resulted in a decreasing sensitivity from  $3.28 \mu\text{A}/\text{mM}$  to  $0.43 \mu\text{A}/\text{mM}$  for a 3 mm diameter electrode. The relative standard deviation in the sensitivity values increased from 2.5% for the sensors with no membrane to 25% for the sensors with the membrane. The PVC membrane did not eliminate the interference of the salt (NaCl tested) with the sensor response (Fig. S6).

### III. OUTLOOK

We describe the optimization and fabrication of a flexible sensing platform to monitor lactate, Na<sup>+</sup>, and NH<sub>4</sub><sup>+</sup> ions in sweat based on the electrochemical sensing. We demonstrated the effect of a diffusion-limiting PVC membrane when implemented in a TTF mediated LOx based working electrode on the sensor performance. Such a membrane would be critical in applications where a wearable sweat sensor needs to be placed directly onto the skin to perform continuous measurements of lactate. This is because the variations in the sweat rate might lead to variations in the transport rate of the lactate to the electrode surface, and hence, causing variations in the sensor readout. The membrane ensures that the sensor response is unaffected by the motion of sweat since diffusion within the membrane is significantly lower than the external diffusion. Incorporating the membrane resulted in a decrease in sensitivity from  $3.28 \mu\text{A}/\text{mM}$  to  $0.43 \mu\text{A}/\text{mM}$  for a 3 mm diameter electrode. This is expected because



the addition of a membrane decreases the transport rate of lactate to the electrode. Incorporating the membrane also led to variability in sensor performance. The relative standard deviation in the sensitivity values increased from 2.5% for the sensors with no membrane to 25% for the sensors with the membrane. The possible reason for the variability is the difference in the membrane morphology between devices that leads to variability in the transport characteristics of the membrane, and consequently, to variability in sensor performance. Additionally, the PVC membrane did not eliminate the interference of the salt (NaCl tested) with the sensor response.

Potentiometric sensors rely on a reference electrode that is insensitive to the changes in Cl concentration. Such printed reference electrodes were previously realized by depositing a polymeric membrane saturated with a chloride salt on top of the Ag/AgCl layer. However, we did not achieve a stable sensor performance through this method, likely due to the diffusion of the chloride ions from the membrane into the solution. We addressed this issue by incorporating the CNT layer between the membrane and the Ag/AgCl layer to act as a surface for the adsorption and retention of Cl<sup>-</sup>. This modification led to a stable, reproducible reference electrode. Coupling the reference electrode with ISEs for Na<sup>+</sup> and NH<sub>4</sub><sup>+</sup> enabled printed wearable potentiometric sensors with a near-Nernstian response. After incorporating 2% weight fraction of CNTs and tuning ionophore content in the sensing membrane, the potentiometric sensors had sensitivities of 60.0 ± 4.0 mV (N = 7) and 56.1 ± 2.2 mV (N = 8) per decade of concentrations for Na<sup>+</sup> and NH<sub>4</sub><sup>+</sup> sensors, respectively. Both sensors showed a stable response after 25 min of conditioning in 50 mM NaCl and 1 mM NH<sub>4</sub>Cl solutions before measuring. Furthermore, the sensors were stable for at least 60 min of operation.

Thus, potentiometric Na<sup>+</sup> and NH<sub>4</sub><sup>+</sup> sensors described in this work demonstrated fast response, sensitivity to physiologically relevant concentrations of analytes found in human sweat, reproducibility, insensitivity to other analytes present in sweat, and, importantly, stable performance under continuous operation for at least 1 h– (approximate duration of the exercise). Future work includes on-body measurements and long-term storage studies. The lactate sensors, on the other hand, require addressing the issue of interference with salts found in sweat, as well as reproducibility of sensors with diffusion limiting membrane before performing the on-body measurements.

#### IV. EXPERIMENTAL SECTION

Selectophore™ grade sodium ionophore X, bis(2-ethylhexyl) sebacate (DOS), sodium tetrakis[3,5-bis(trifluoromethyl)phenyl] borate (Na-TFPB), polyvinyl chloride (PVC), tetrahydrofuran (THF), polyvinyl butyral, analytical grade salts of ammonium chloride and sodium chloride (99.5%), nonactin (ammonium ionophore I), 2-nitro-phenyl-octyl ether (*o*-NPOE) with >99% purity, chitosan, acetone, ethanol, uric acid, ascorbic acid, glucose, creatinine, and acetic acid were obtained from Sigma Aldrich. Lactate oxidase was obtained from Toyobo. Carbon nanotubes were obtained from Carbon Solutions, Inc., in the form of iP-Single Walled Carbon Nanotubes. A pH 7.0 buffer was obtained from Fisher Scientific.

Gold electrodes were inkjet-printed using Harima Nanopaste (Au) NPG-J gold ink in a Dimatix inkjet printer at ambient

conditions. The resulting gold electrodes were annealed at 250 °C for 50 min. Ag/AgCl was screen-printed using Engineered Materials Systems, Inc., CI-4001 ink. After printing, the Ag/AgCl electrodes were baked at 110 °C in a vacuum oven for 2 h. The electrodes were printed on 25 μm thick PEN substrates. Printed electrodes were encapsulated using a laser-cut Teflon tape. The tape insulated the conductive traces that lead to circuitry connections and ensured that the sensor components deposited from the solution were contained within the circular areas of 3 mm diameter (area of 0.07068 cm<sup>2</sup>). In the case of the potentiometric sensors, an additional layer of carbon nanotubes (CNT) dispersed in THF, followed by PVB/NaCl membrane drop-casted on top of the Ag/AgCl layer. Homogeneous CNT/THF suspension was achieved using the block copolymer PEO-PPO-PEO (F127) as a surfactant. 0.01 g of CNTs and 0.05 g of F127 were dissolved in 10 ml of THF and sonified for one hour in an ice bath using a Branson Digital Sonifier probe set on 15% power. The 4 μl of the mixture was drop-casted in two 2 μl increments on the printed Ag/AgCl electrode surface. The PVB and NaCl membrane were made by dissolving 1.58 g of PVB and 1 g of NaCl in 20 ml of methanol and sonifying the resulting mixture for 30 min in an ice bath at 15% power. 4 μl of the solution was then drop-casted in two 2 μl increments on top of the CNT layer, resulting in the membrane thickness of ~5 μm.

The ammonium-selective membrane solution consisted of 0.2 wt. % of nonactin, 69.0 wt. % of *o*-NPOE, and 30.8 wt. % of PVC, as described elsewhere.<sup>16</sup> The sodium-selective membrane solution consisted of 1 mg sodium ionophore X, 0.55 mg Na-TFPB, 33 mg PVC, and 65.45 mg DOS dissolved in 660 ml of THF.<sup>23</sup>

To make the mediating layer for the lactate sensor, carbon nanotubes were dispersed in ethanol at 1.25 mg/ml and sonified for 20 min at 40% amplitude using a Branson Digital Sonifier probe. Meanwhile, TTF was dissolved in acetone at 25 mg/ml. 400 μl of TTF was added to 2 ml CNT dispersion, and the resulting solution was sonified for 20 min at 40% amplitude. The TTF/CNT dispersion was then deposited on the working electrode surface. To make the enzyme layer, chitosan was dissolved in 1% acetic acid in water (0.6% chitosan by weight for optimized sensors), and CNTs were added (1% by weight for optimized sensors). This mixture was sonified for 20 min at 40% amplitude. In a separate vial, lactate oxidase was measured out and dissolved in Fisher pH 7.0 buffer (for optimized sensors, 1500 U/ml). The lactate oxidase mixture was mixed 1:1 with the chitosan and CNT mixture and deposited on top of the mediating layer (1 drop of 10 μl for optimized sensors). The sensors were then dried overnight in an environmental chamber at 35 °C.

#### SUPPLEMENTARY MATERIAL

See the [supplementary material](#) for the SEM of the screen-printed Ag/AgCl traces, effect of the reference membrane thickness on the potential response, variability in sensitivity with CNT concentration in sensing membrane, Na<sup>+</sup> ISE measurements in sweat, continuous operation of lactate sensor, and calibration curves of the lactate working electrodes with the diffusion limiting membrane.

#### AUTHORS' CONTRIBUTIONS

A.M.Z. and N.A.D.Y. contributed equally to this work.

## ACKNOWLEDGMENTS

This work was based on the work supported, in part, by the National Science Foundation Graduate Research Fellowships Program under Grant No. DGE-1106400.

## DATA AVAILABILITY

The data that support the findings of this study are available from the corresponding author upon reasonable request.

## REFERENCES

- J. Heikenfeld *et al.*, "Wearable sensors: Modalities, challenges, and prospects," *Lab Chip* **18**, 217–248 (2018).
- J. Heikenfeld, "Non-invasive analyte access and sensing through eccrine sweat: Challenges and outlook circa 2016," *Electroanalysis* **28**, 1242–1249 (2016).
- X. Huang *et al.*, "Stretchable, wireless sensors and functional substrates for epidermal characterization of sweat," *Small* **10**, 3083–3090 (2014).
- G. Liu *et al.*, "A wearable conductivity sensor for wireless real-time sweat monitoring," *Sens. Actuators, B* **227**, 35–42 (2016).
- J. Choi, D. Kang, S. Han, S. B. Kim, and J. A. Rogers, "Thin, soft, skin-mounted microfluidic networks with capillary bursting valves for chrono-sampling of sweat," *Adv. Healthcare Mater.* **6**, 1601355 (2017).
- A. Koh *et al.*, "A soft, wearable microfluidic device for the capture, storage, and colorimetric sensing of sweat," *Sci. Transl. Med.* **8**, 366ra165 (2016).
- J. R. Sempionatto *et al.*, "Skin-worn soft microfluidic potentiometric detection system," *Electroanalysis* **31**, 239–245 (2019).
- H. Y. Y. Nyein *et al.*, "Regional and correlative sweat analysis using high-throughput microfluidic sensing patches toward decoding sweat," *Sci. Adv.* **5**, eaaw9906 (2019).
- Z. Yuan *et al.*, "A multi-modal sweat sensing patch for cross-verification of sweat rate, total ionic charge, and Na<sup>+</sup> concentration," *Lab Chip* **19**, 3179–3189 (2019).
- D. Morris *et al.*, "Bio-sensing textile based patch with integrated optical detection system for sweat monitoring," *Sens. Actuators, B* **139**, 231–236 (2009).
- M. Singh, J. Truong, W. B. Reeves, and J.-I. Hahm, "Emerging cytokine biosensors with optical detection modalities and nanomaterial-enabled signal enhancement," *Sensors* **17**, 428 (2017).
- A. J. Bandodkar and J. Wang, "Non-invasive wearable electrochemical sensors: A review," *Trends Biotechnol.* **32**, 363–371 (2014).
- M. M. Raiszadeh *et al.*, "Proteomic analysis of eccrine sweat: Implications for the discovery of schizophrenia biomarker proteins," *J. Proteome Res.* **11**, 2127–2139 (2012).
- M. Bariya, H. Y. Y. Nyein, and A. Javey, "Wearable sweat sensors," *Nat. Electron.* **1**, 160–171 (2018).
- W. Jia *et al.*, "Electrochemical tattoo biosensors for real-time noninvasive lactate monitoring in human perspiration," *Anal. Chem.* **85**, 6553–6560 (2013).
- T. Guinovart, A. J. Bandodkar, J. R. Windmiller, F. J. Andrade, and J. Wang, "A potentiometric tattoo sensor for monitoring ammonium in sweat," *Analyst* **138**, 7031–7038 (2013).
- B. Schazmann *et al.*, "A wearable electrochemical sensor for the real-time measurement of sweat sodium concentration," *Anal. Methods* **2**, 342 (2010).
- J. Kim *et al.*, "Noninvasive alcohol monitoring using a wearable tattoo-based iontophoretic-biosensing system," *ACS Sensors* **1**, 1011–1019 (2016).
- Y. Lin *et al.*, "Porous enzymatic membrane for nanotextured glucose sweat sensors with high stability toward reliable noninvasive health monitoring," *Adv. Funct. Mater.* **29**, 1902521 (2019).
- J. Kim *et al.*, "Wearable temporary tattoo sensor for real-time trace metal monitoring in human sweat," *Electrochem. Commun.* **51**, 41–45 (2015).
- M. Barbadillo *et al.*, "Gold nanoparticles-induced enhancement of the analytical response of an electrochemical biosensor based on an organic-inorganic hybrid composite material," *Talanta* **80**, 797–802 (2009).
- J. M. Goran, J. L. Lyon, and K. J. Stevenson, "Amperometric detection of L-lactate using nitrogen-doped carbon nanotubes modified with lactate oxidase," *Anal. Chem.* **83**, 8123–8129 (2011).
- A. J. Bandodkar *et al.*, "Epidermal tattoo potentiometric sodium sensors with wireless signal transduction for continuous non-invasive sweat monitoring," *Biosens. Bioelectron.* **54**, 603–609 (2014).
- J. Zhao *et al.*, "A fully integrated and self-powered smartwatch for continuous sweat glucose monitoring," *ACS Sensors* **4**, 1925–1933 (2019).
- S. Anastasova *et al.*, "A wearable multisensing patch for continuous sweat monitoring," *Biosens. Bioelectron.* **93**, 139–145 (2017).
- D. Rose *et al.*, "Adhesive RFID sensor patch for monitoring of sweat electrolytes," *IEEE Trans. Biomed. Eng.* **62**, 1457–1465 (2014).
- S. Emaminejad *et al.*, "Autonomous sweat extraction and analysis applied to cystic fibrosis and glucose monitoring using a fully integrated wearable platform," *Proc. Natl. Acad. Sci. U. S. A.* **114**, 4625–4630 (2017).
- H. Y. Y. Nyein *et al.*, "A wearable electrochemical platform for noninvasive simultaneous monitoring of Ca<sup>2+</sup> and pH," *ACS Nano* **10**, 7216–7224 (2016).
- W. Gao *et al.*, "Fully integrated wearable sensor arrays for multiplexed in situ perspiration analysis," *Nature* **529**, 509–514 (2016).
- S. Imani *et al.*, "A wearable chemical–electrophysiological hybrid biosensing system for real-time health and fitness monitoring," *Nat. Commun.* **7**, 11650 (2016).
- M. F. Bergeron, "Heat cramps: Fluid and electrolyte challenges during tennis in the heat," *J. Sci. Med. Sport* **6**, 19–27 (2003).
- R. A. Robergs, F. Ghiasvand, and D. Parker, "Biochemistry of exercise-induced metabolic acidosis," *Am. J. Physiol.: Regul., Integr. Comp. Physiol.* **287**, R502–R516 (2004).
- P. J. Derbyshire, H. Barr, F. Davis, and S. P. J. Higson, "Lactate in human sweat: A critical review of research to the present day," *J. Physiol. Sci.* **62**, 429–440 (2012).
- Z. Sonner *et al.*, "The microfluidics of the eccrine sweat gland, including biomarker partitioning, transport, and biosensing implications," *Biomicrofluidics* **9**, 031301 (2015).
- D. Czarnowski, J. Langfort, W. Pilis, and J. Gorski, "Effect of a low-carbohydrate diet on plasma and sweat ammonia concentrations during prolonged nonexhausting exercise," *Eur. J. Appl. Physiol. Occup. Physiol.* **70**, 70–74 (1995).
- D. Czarnowski, J. Górski, J. Józwiuk, and A. Boroń-Kaczmarek, "Plasma ammonia is the principal source of ammonia in sweat," *Eur. J. Appl. Physiol. Occup. Physiol.* **65**, 135–137 (1992).
- A. Moya *et al.*, "Stable full-inkjet-printed solid-state Ag/AgCl reference electrode," *Anal. Chem.* **91**, 15539–15546 (2019).
- T. Guinovart, G. A. Crespo, F. X. Rius, and F. J. Andrade, "A reference electrode based on polyvinyl butyral (PVB) polymer for decentralized chemical measurements," *Anal. Chim. Acta* **821**, 72–80 (2014).
- J. Ha *et al.*, "A polymeric junction membrane for solid-state reference electrodes," *Anal. Chim. Acta* **549**, 59–66 (2005).
- N.-H. Kwon, K.-S. Lee, M.-S. Won, and Y.-B. Shim, "An all-solid-state reference electrode based on the layer-by-layer polymer coating," *Analyst* **132**, 906–912 (2007).
- K. Idegami, M. Chikae, N. Nagatani, E. Tamiya, and Y. Takamura, "Fabrication and characterization of planar screen-printed Ag/AgCl reference electrode for disposable sensor strip," *Jpn. J. Appl. Phys., Part 1* **49**, 097003 (2010).
- U. Guth, F. Gerlach, M. Decker, W. Oelßner, and W. Vonau, "Solid-state reference electrodes for potentiometric sensors," *J. Solid State Electrochem.* **13**, 27–39 (2009).
- S. Wang *et al.*, "Highly stretchable potentiometric ion sensor based on surface strain redistributed fiber for sweat monitoring," *Talanta* **214**, 120869 (2020).
- W. He *et al.*, "Integrated textile sensor patch for real-time and multiplex sweat analysis," *Sci. Adv.* **5**, eaax0649 (2019).
- M. Parrilla, J. Ferré, T. Guinovart, and F. J. Andrade, "Wearable potentiometric sensors based on commercial carbon fibres for monitoring sodium in sweat," *Electroanalysis* **28**, 1267–1275 (2016).

- <sup>46</sup>S. Y. Oh *et al.*, "Skin-attachable, stretchable electrochemical sweat sensor for glucose and pH detection," *ACS Appl. Mater. Interfaces* **10**, 13729–13740 (2018).
- <sup>47</sup>M. Bariya *et al.*, "Roll-to-roll gravure printed electrochemical sensors for wearable and medical devices," *ACS Nano* **12**, 6978–6987 (2018).
- <sup>48</sup>G. A. Crespo, S. Macho, and F. X. Rius, "Ion-selective electrodes using carbon nanotubes as ion-to-electron transducers," *Anal. Chem.* **80**, 1316–1322 (2008).
- <sup>49</sup>E. J. Parra, G. A. Crespo, J. Riu, and F. X. Rius, "Ion-selective electrodes using multi-walled carbon nanotubes as ion-to-electron transducers for the detection of perchlorate," *Analyst* **134**, 1905–1910 (2009).
- <sup>50</sup>M. Parrilla *et al.*, "Wearable potentiometric ion patch for on-body electrolyte monitoring in sweat: Toward a validation strategy to ensure physiological relevance," *Anal. Chem.* **91**, 8644–8651 (2019).
- <sup>51</sup>A. J. Bard and L. R. Faulkner, *Electrochemical Methods: Fundamentals and Applications* (Wiley, 2001).
- <sup>52</sup>M. Alvarez-Icaza and U. Bilitewski, "Mass production of biosensors," *Anal. Chem.* **65**, 525A–533A (1993).
- <sup>53</sup>M. E. Payne, A. Zamarayeva, V. I. Pister, N. A. D. Yamamoto, and A. C. Arias, "Printed, flexible lactate sensors: Design considerations before performing on-body measurements," *Sci. Rep.* **9**, 13720 (2019).
- <sup>54</sup>A. Weltin *et al.*, "Polymer-based, flexible glutamate and lactate microsensors for *in vivo* applications," *Biosens. Bioelectron.* **61**, 192–199 (2014).
- <sup>55</sup>H. Liu and J. Deng, "An amperometric lactate sensor employing tetrathiafulvalene in Nafion film as electron shuttle," *Electrochim. Acta* **40**, 1845–1849 (1995).
- <sup>56</sup>B. Kowalewska and P. J. Kulesza, "Application of tetrathiafulvalene-modified carbon nanotubes to preparation of integrated mediating system for bioelectrocatalytic oxidation of glucose," *Electroanalysis* **21**, 351–359 (2009).
- <sup>57</sup>A. Mulchandani, A. S. Bassi, and A. Nguyen, "Tetrathiafulvalene-mediated biosensor for L-lactate in dairy products," *J. Food Sci.* **60**, 74–78 (1995).
- <sup>58</sup>K. Rathee, V. Dhull, R. Dhull, and S. Singh, "Biosensors based on electrochemical lactate detection: A comprehensive review," *Biochem. Biophys. Rep.* **5**, 35–54 (2016).